

# Statistical survey of UV compact bursts observed by IRIS

M. Litwicka<sup>(1)</sup>, A. Berlicki<sup>(2)</sup>, B. Schmieder<sup>(3)</sup>

(1) Space Research Centre Polish Academy of Sciences, WROCLAW, POLAND (2) Astronomical Institute, University of Wrocław, POLAND, (3) Observatoire de Paris-Meudon, LESIA, FRANCE



## ABSTRACT

UV compact bursts (CBs) are frequently observed by IRIS in both NUV and FUV channels. They appear as small and intense short lifetime brightenings visible in solar active regions. Some of them can be closely connected with well-known Ellerman bombs and IRIS bombs. In this novel work we present statistical survey of compact bursts observed in active regions with emerging flux areas, sunspots and plages. Our analysis is based on the IRIS observations in Mg II h and k lines in NUV band as well as in Si IV and C II transition region lines in FUV band. We used only dense and large rasters for searching of compact bursts with the size of the order of 1". We found 2053 compact bursts in 170 such rasters. Only brightenings with the intensity contrast greater than 2 in Mg II h line wings at -3.5Å (2800Å), and greater than 9 in case of integrated and averaged intensity of the Mg II k line, in the range -1.25, +1.25Å were analysed. In addition, only brightenings with the contrast greater than 6.5 in the Mg II k line and simultaneously greater than 1.5 at 2800Å were taken into account. Using Mg II h and k line profiles for all brightening we run statistical analysis of some parameters of the line profiles: peak separation, peak ratio, line centre intensity, contrast in characteristic profiles points and FWHM. In addition we analysed also intensity of Mg II UV triplet and some parameters of Si IV and C II lines. This analysis allows us to categorise bursts in the way as it was done in Grubecka et al. (2016). We also searched for correlations between the emission of Mg II lines and hotter Si IV line in order to find which of events are linked with solar ultraviolet burst (UV burst, Young et al. 2018). Finally, we analysed and defined the observing parameters of those CBs, which can be associated with Ellerman bombs.

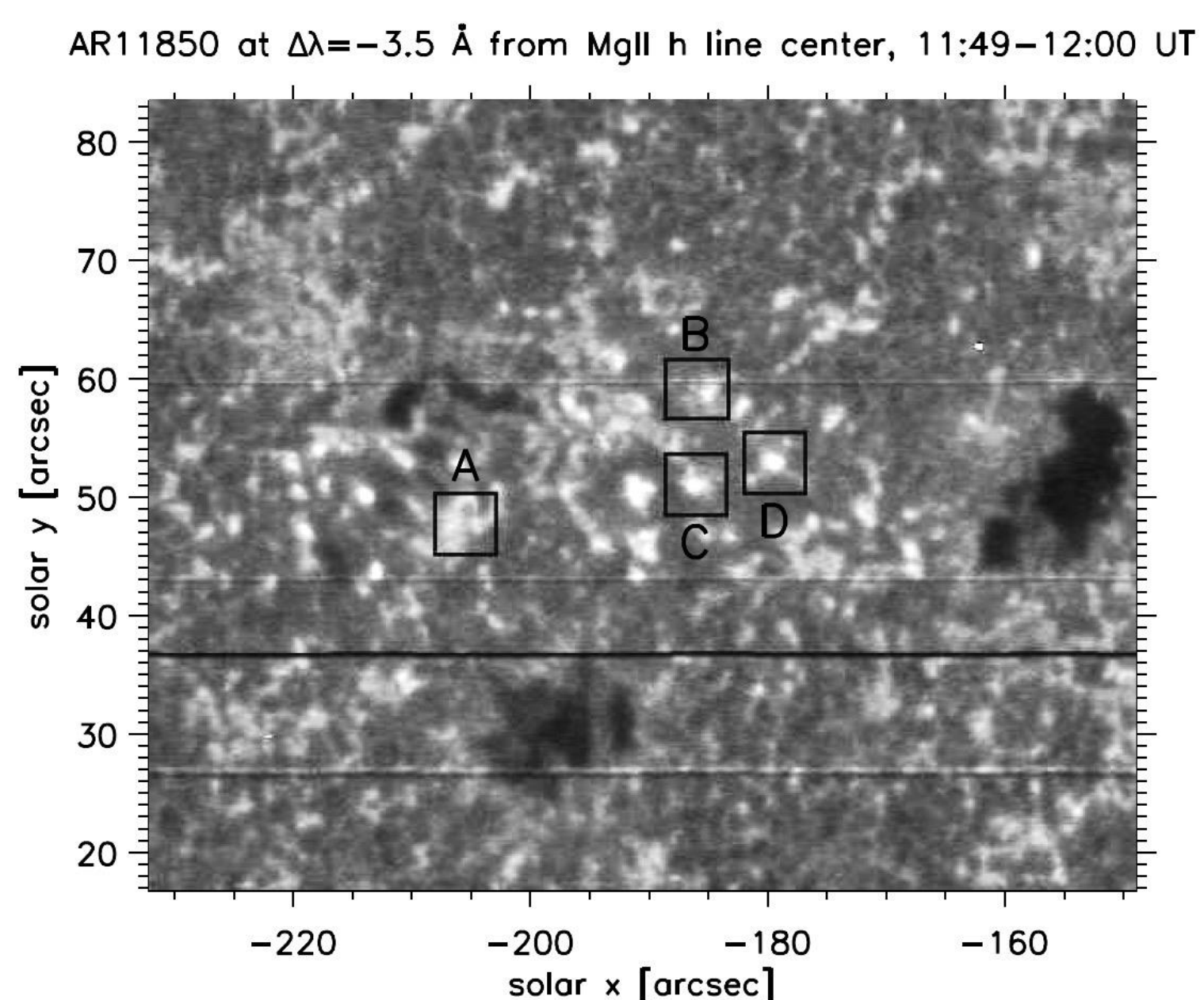


Fig. 1: IRIS observations of the AR 11850 - spectroheliograms in the Mg II line wing reconstructed at 2800.0 Å (from Grubecka et al. 2016). Several CBs visible in the FOV.

Our interest in CBs was initiated by the paper Grubecka et al. 2016, in which we modelled 5 different selected compact bursts visible in Mg II h and k lines. The diversity and possible connection of CBs with Ellerman Bombs, IRIS bombs (IBs) and both simultaneously is also analysed in this current work.

Our present aims is to investigate statistically diversity of Mg II h and k lines of compact phenomena (CBs) and its visibility in far UV lines such as Si IV, C II and in Mg II triplet. In order to achieve goals, in IRIS database we searched for dense rasters of active and emerging flux region containing spectra in Mg II, C II, Si IV.

## ANALYSIS AND CORRELATIONS BETWEEN PROFILES PARAMETERS

Parameter	Type 1	Type 2	Type 3
$C_C$	9,03	3,89	1,16
$C_P$	9,35	4,07	1,68
$C_L$	12,64	4,58	1,89
$C_{+1\text{Å}}$	6,21	2,96	2,37
$C_{2800\text{Å}}$	1,28	2,46	2,50
$C_{TW}$	2,69	3,01	2,67
$C_{TL}$	3,80	1,67	0,88
$FWHM$	0,91	0,58	0,54

Table 1. Average values of contrast parameters presented for each type of CBs separately.

Histograms show how parameters value are distributed between three types of CBs. Visual inspection among particular types revealed additional characteristics. CBs from type 3 are very similar and differs between each other only in details. The biggest diversity presents CBs of type 1.

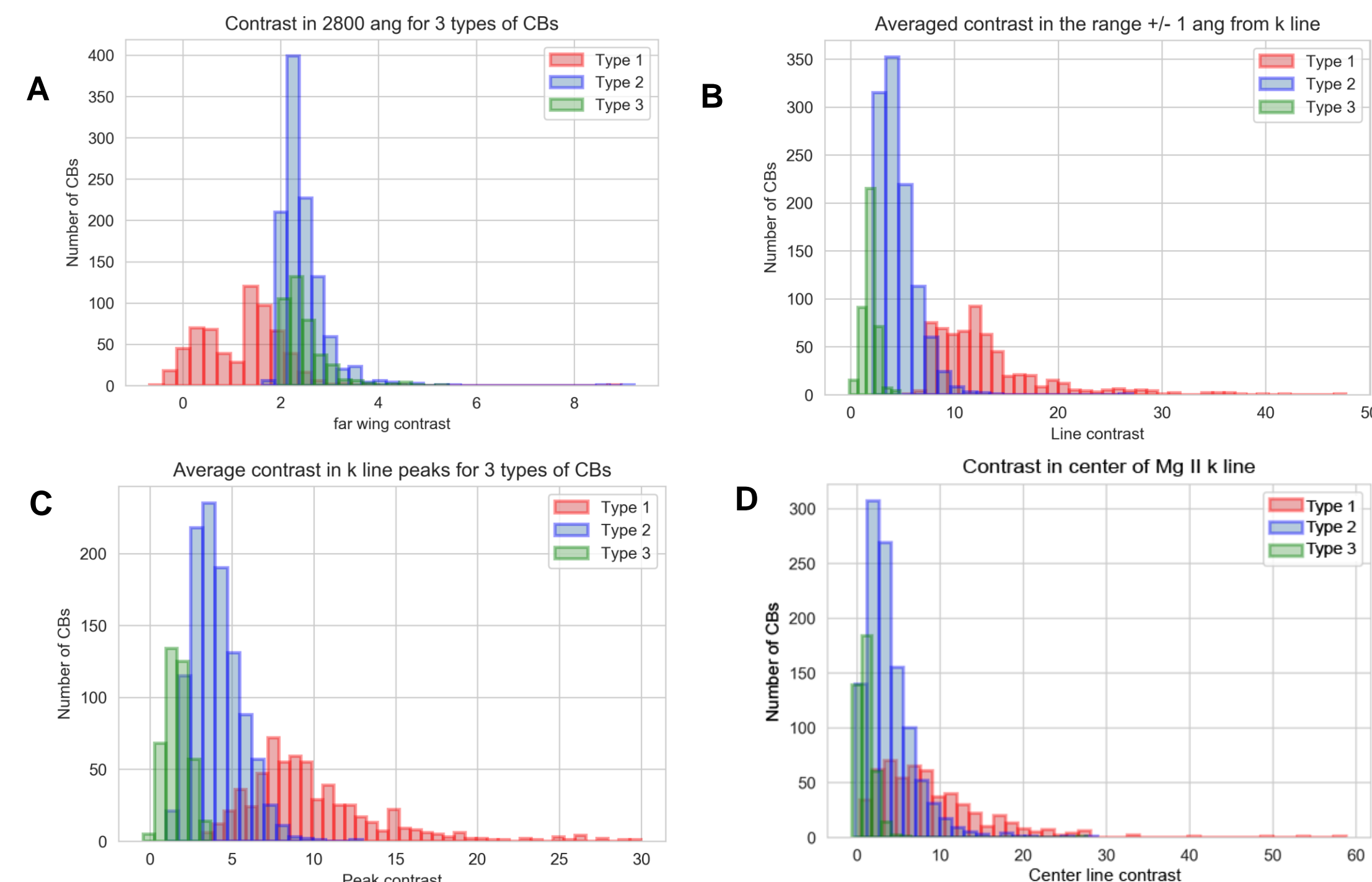


Fig. 5: Histograms of three contrast parameters: at 2800Å (A), of Mg II k line integrated intensity (B), at peaks of Mg II k line (C) and histogram of contrast in center of Mg II k line (D). The contrast was calculated with respect to the QS according to the formula:  $C = (I_{CB} - I_{QS})/I_{QS}$

## IRIS DENSE AND LARGE RASTERS

For our analysis we used 170 dense rasters observed between 2013 and 2018. Dense rasters are necessary to have good spatial coverage of small scale CBs.

We constitute 3 search criteria for searching algorithm based on contrast in different wavelengths and the automatic procedure found 2950 compact bursts (CBs) in 170 rasters. These 3 searching criteria can be summarized:

- 1) brightenings with greater than 2 contrast at 2800Å: **1835 EVENTS FOUND**
- 2) brightenings with greater than 9 contrast in integrated and averaged intensity of Mg II k line in range -1.25, +1.25 Å): **499 EVENTS FOUND**
- 3) brightenings with greater than 6.5 contrast in Mg II k line and simultaneously greater than 1.5 contrast at 2800Å: **616 EVENTS FOUND**

To obtain contrast we need values for quiet Sun intensity. For each raster we determined the area of the Sun surface where the smallest intensity was observed with no activity structures. Then we calculated average Mg II h and k profile for whole quiet Sun area.

Next step was to verify brightenings based on spectra and profiles in the context of:

- cosmic rays
- compact structure and size
- repeated events
- phenomena consider as micro-flare type events

After the verification of automatically found 2950 CBs we accepted 2053 CBs for further analysis

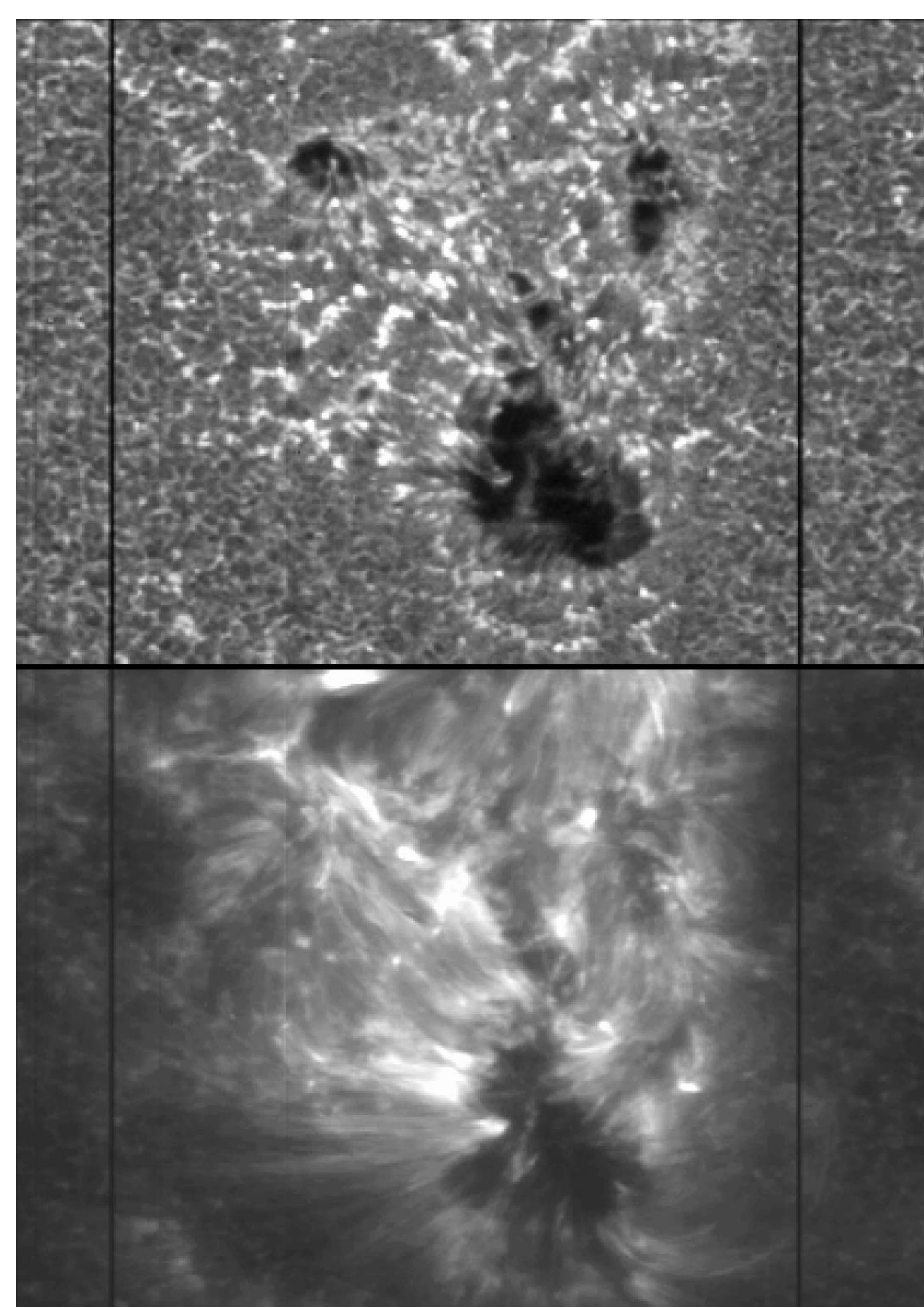


Fig. 2: Examples of IRIS dense rasters of one active region area observed on February 4th, 2016. This AR presented one of the biggest collection of CBs. Top image is reconstructed at 2800 Å, bottom one represents integrated Mg II k line intensity integrated within +/- 1 Å range.

## OCCURRENCE OF CBS IN DIFFERENT TYPES OF ACTIVE REGIONS

Among 170 rasters analyzed in our work there were different types of active regions. We determined 4 main types: emerging flux region (EMF), areas close to the penumbra sunspot, plage region and so-called isolated CBs. When active region showed to have signatures of more than one type of the region, then each CBs from this region was classified to different type. Emerging flux region was area with strong bi-polar magnetic field visible on HMI magnetograms. Plages were hot and wide area with no other structures. Sunspot area CBs were located around (up to 1 radius) sunspot, close or in penumbra. Isolated CBs were distant from other events in region with no characteristic active structure surrounded. Our goal was examination what kind of active regions produce greater number of CBs and what is the dominant type of CBs. Figure 6 presents the number of brightenings of different types observed in different types of active regions.

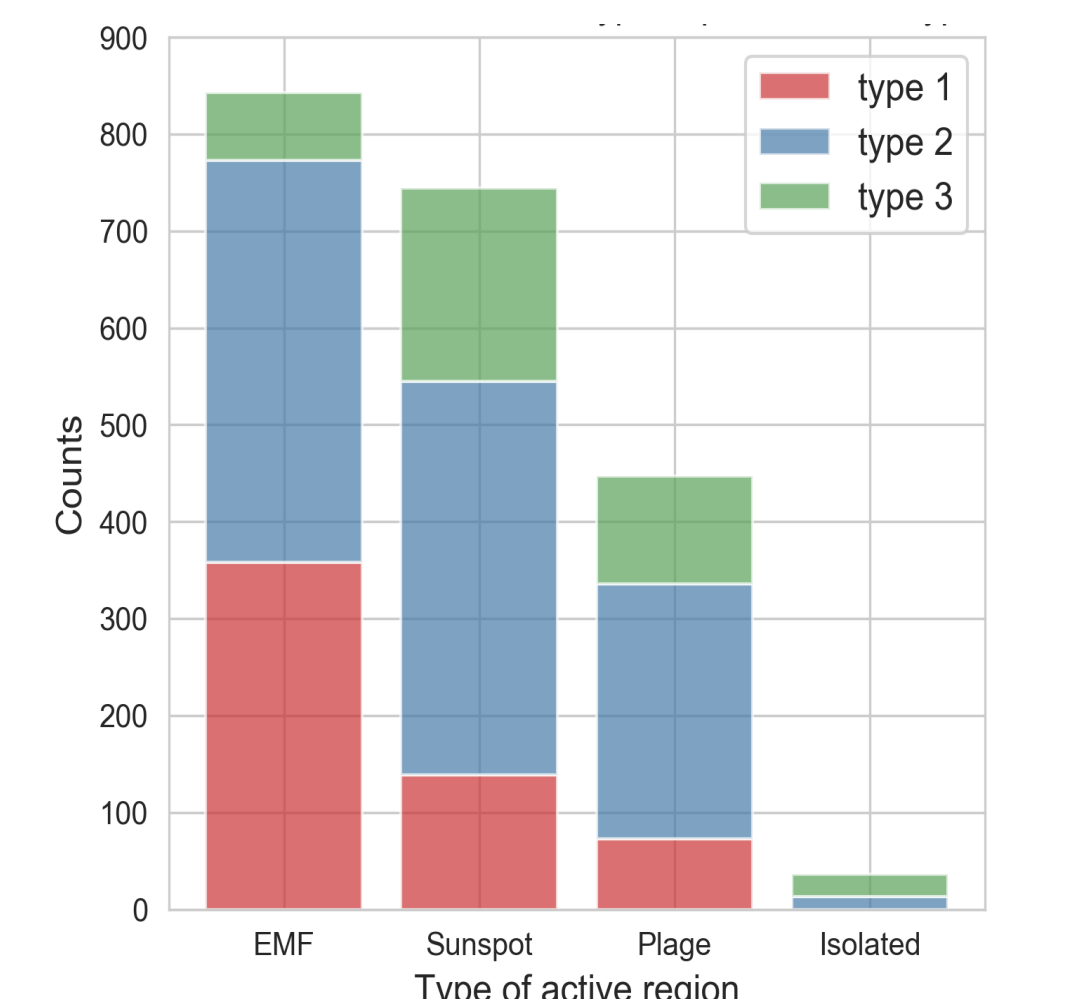


Fig. 6

	EMF	Sunspot	Plage	Isolated
FWHM	0.75	0.61	0.60	0.50
Triplet emission	41 %	31 %	17 %	0 %
Si IV emission	18.2	9.3 %	5.8 %	0.5

Table 2

As we can notice, emerging flux regions are those areas, where CBs occurs the most often, 827 events come from EMF. In sunspot areas we count 744 CBs and in plages 446 CBs. Only 36 of phenomena were isolated from active structures in ARs. From Table 2 we can see that emerging flux region produced more energetic events, with broader line profiles, stronger triplet and FUV emission.

## MG II TRIPLET

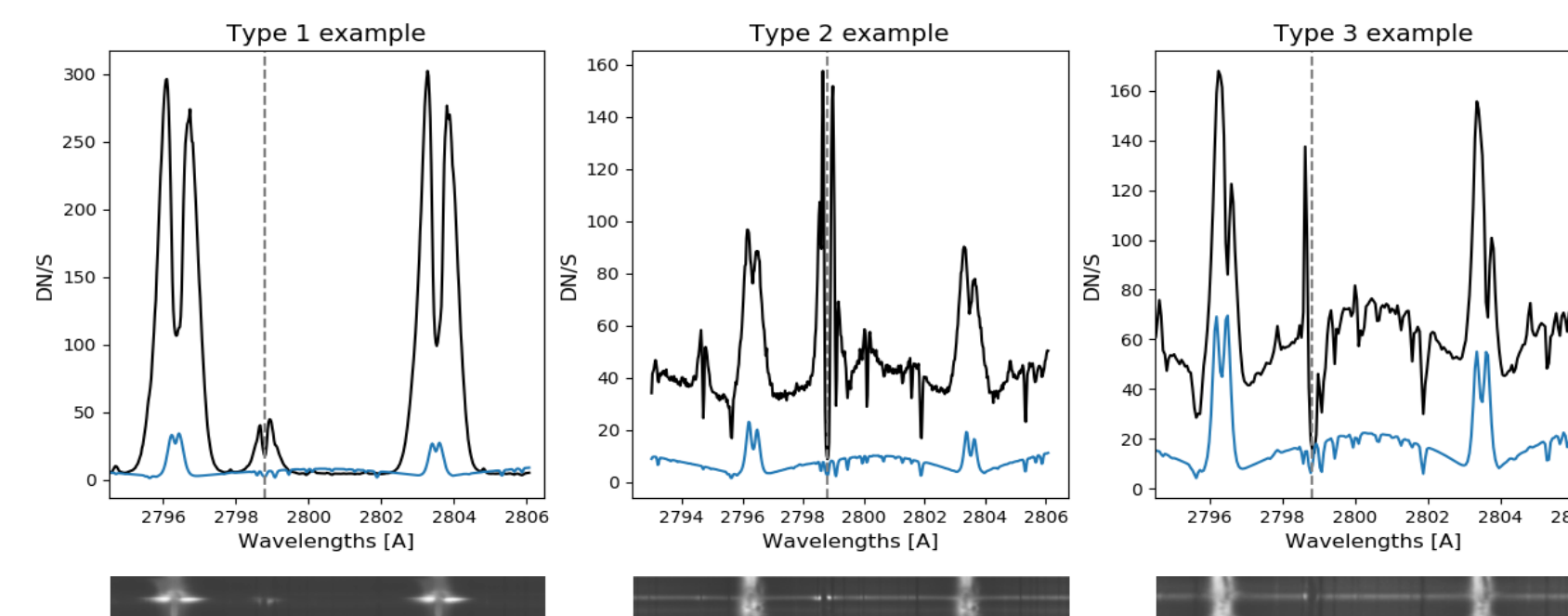


Fig. 7: Examples of CBs events with strong emission in Mg II UV triplet.

Triplet Mg II UV emission in 2798.8 Å line occurs mainly for strong CBs events with strong emission in h and k lines (strong peaks), but not for events with emission only in far wings. Around 72% of CBs of Type 1 exhibit also increased emission in Mg II triplet. For Type 2 it is 43%, and for Type 3 only 28% of CBs show strong emission in Mg II triplet.

## PARAMETERS OF THE MG II K LINE AND CLASSIFICATION OF COMPACT BURSTS

First step was to calculate for each Mg II line profiles a set of parameters (metrics), which help us define, describe and compare each events. All parameters were calculated for k line (some of raster have only spectral range around k line)

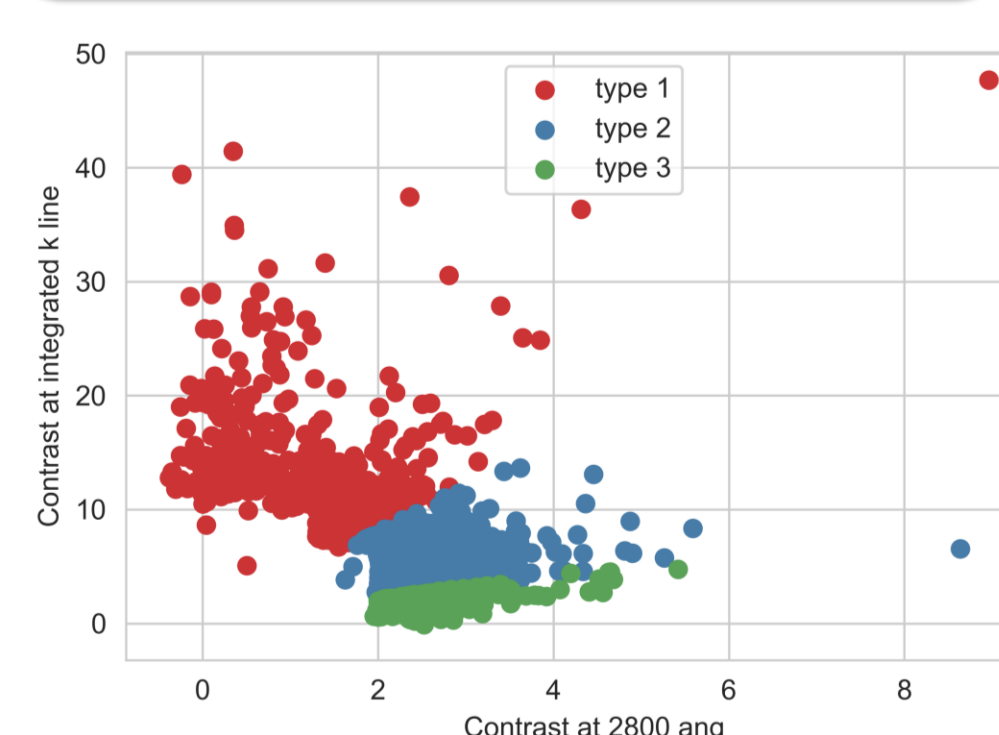


Fig. 3: Distribution plot of CBs parameters  $C_{2800\text{Å}}$  and  $C_L$ . Different colors refers to different type of CBs.

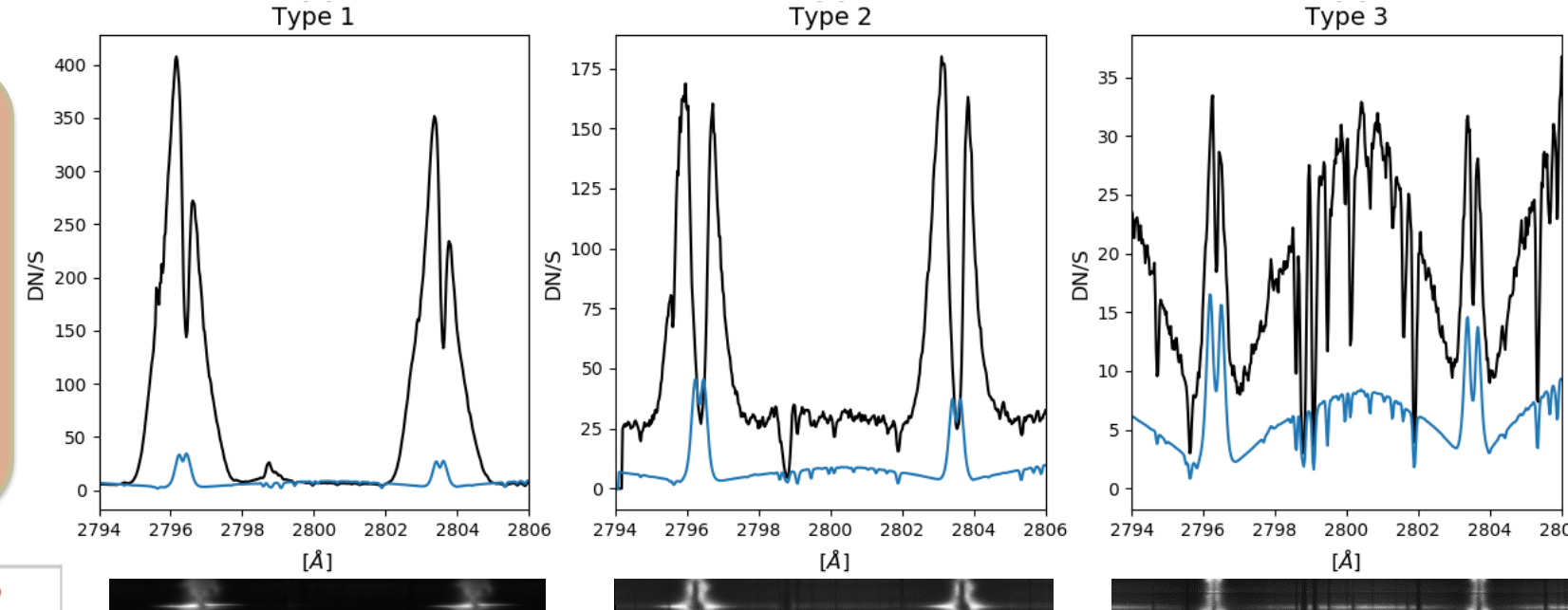


Fig. 4: Examples of different type CBs, profiles and spectra.

### Analyzed parameters:

- $C_C$  - Line center intensity contrast
- $C_P$  - Peak intensity contrast
- $C_L$  - Line integrated intensity contrast
- $C_{+1\text{Å}}$  - Contrast at +1 Å from k line
- $C_{2800\text{Å}}$  - Contrast at 2800 Å
- $C_{TW}$  - Average contrast at wing of Mg II UV triplet
- $C_{TL}$  - Contrast at center Mg II UV triplet
- $FWHM$  - full width at half maximum of k line

Referring to our previous paper Grubecka et al. 2016, where we made a first step in classification of observing Mg II h and k profiles of CBs, we divided them in 3 types in the following way:

- Type 1** - CBs with strong emission only in Mg II line peaks or in line center;
- Type 2** - CBs with emission observed both in the line peaks and line wings (emission raised in the whole spectral range);
- Type 3** - CBs showing emission only in far wings of Mg II h and k lines

Our classification of CBs is based on the relation between emission in the wing of k line (at 2800Å) and emission in the k line in the range 2795.35-2797.35Å ( $C_{2800\text{Å}} / C_L$ ). This division reflects formation heights. Figure 3 presents distribution plot of two CBs parameters  $C_{2800\text{Å}}$  and  $C_L$ .

We found that 27% (556) of CBs belong to Type 1, 53% (1096) to Type 2 and 20% (401) to Type 3. In figure 4 we present some examples of the Mg II k profiles and spectra for CBs of all three types.

Vissers et al. 2015, Tian et al. 2016 presented evidences for emission both in Mg II h and k lines and in Si IV, with suggestion that this simultaneous emission appears only for strong events. Our goal is to investigate for which events, especially for which type of them we can observe simultaneous emission in Mg II, Si IV and C II line.

From our 2053 CBs, 879 (43%) have emission in Si IV line and 1380 (67%) show response in C II lines.

Fraction of CBs with emission in FUV differ among types:

**Type 1:** 91% of CBs have emission in Si IV and 99% in CII  
**Type 2:** 31% of CBs have emission in Si IV and 66% in CII  
**Type 3:** 8% of CBs have emission in Si IV and 26% in CII

Based on Tian et al. 2016, Young et al. 2018, we determined how many CBs are IRIS bombs (IBs), UV Burst and Ellerman Bombs (EBs). Among 2053 CBs we found 49 IBs, 125 UV burst and 273 EBs. We found that:

- 29 CBs are EBs and IBs simultaneously, which is 10.6% of EBs and 59% of IBs
- 51 CBs are EBs and UV burst simultaneously, which is 19% of EBs and 41% of UV burst.

## SI IV AND C II EMISSION

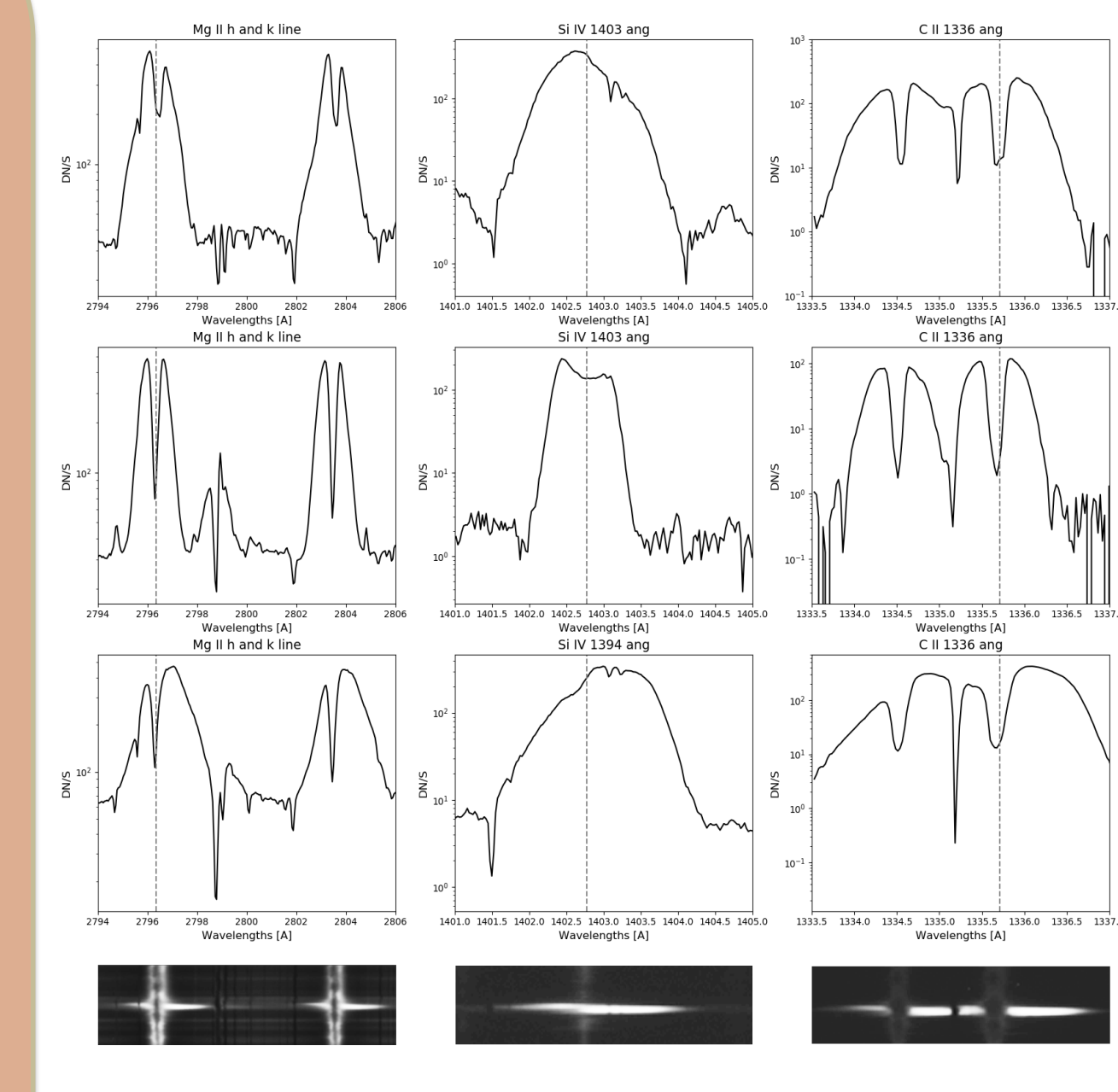


Fig. 8: Examples of 3 IBs-EBs events in Mg II h&k, Si IV and C II line. Spectra below plots refers to 3rd events example (bottom panel).

## SUMMARY AND PRELIMINARY CONCLUSIONS

In this preliminary work we analyzed basic characteristics of 2053 CBs. In particular, the relations between Mg II and hotter Si IV and C II lines were analyzed. CBs with strong emission in Mg II most often has also strong emission in Si IV and C II. This suggests that CBs located higher in solar atmosphere affect also the TR plasma. It is interesting to notice that there is group of CBs with strong Mg II emission without any emission in FUV lines, which makes problem of CBs formation even more complicated. The 3 types of CBs defined in our work represent not only different shapes of Mg II line profiles, but also different formation heights. Our results of modeling of Ellerman Bombs (Grubecka et al. 2016) showed some dependence between Mg II spectrum and the formation height: type 1st is forming above temperature minimum region, type 2nd exactly in temperature minimum region and last 3rd type below this area. Theoretical modelling of the lines observed in CBs will provide a better constraints on the temperature, plasma density and dynamics of CBs.

### References

- Young P. R. et al. 2018, Space Science Reviews, 214, 8, 120
- Grubecka, M., Schmieder, B., Berlicki, A., Heinzel, P., Dalmasse, K., Mein, P. 2016, A&A, 593, 32
- Tian, H., Xu, Z., He, J., Madsen, C. 2016, 824, 96
- Vissers, G. J. M., Rouppe van der Voort, L. H. M., Rutten, R. J., Carlsson, M., De Pontieu, B. 2015, ApJ, 812, 11